A Numerical Variational Approach for Rotor-Propeller Aerodynamics in Axial Flight

F. Simonetti[1], **R. M. Ardito Marretta**[2]

Abstract: Advanced propellers are being developed to improve the performance and fuel economy of future transport aircraft. To study them, various aerodynamic prediction models and systems (from theory to experiment) have been developed via several approaches (Free Wake Analysis, helicoidal source methods, scale model tests). This study focuses on the development of an efficient numerical method to predict the behaviour of rotor or propeller in forward flight. Based on a variational approach, the present numerical technique allows a significant reduction of computer resources used in the calculation of instantaneous velocities to determine the wake geometry and the three-dimensional vortex flow streaming back from the propeller. Wind tunnel test data are presented to substantiate the theory and to show its limitations. The analytical structure of the model is described and its capability is analyzed by a numerical simulation checked against available with experimental data obtained on a scale model of a four-bladed propeller. Assuming the hypothesis of incompressible flow, the simulation results show a very good agreement with experiments for a wide range of operating parameters.

keyword: variational numerical scheme, propeller wake

Nomenclature

b: number of blades
c: local chord, m
C: vortex path
c_d: drug coefficient
c_l: lift coefficient
F, Q: thrust and torque of the propeller, N, Nm
G: influence function
j: operating parameter $V_\infty \pi/\omega r_1$
n_q: number of elements of $\mathbf{q}$
N: shape matrix
$Ox_1x_2x_3$: fixed coordinate system defined in Fig.1
$\mathbf{q}$: vector of unknown parameters
r_0, r_1: hub and blade radii, m
T: versor tangent to the vortex line
u, v, w: induced velocity components shown in Fig.1, m/s
V_∞: freestream axial velocity, m/s
$\mathbf{V}$: induced vector velocity
$\mathbf{x}$, $\mathbf{y}$: vectors of the space $Ox_1x_2x_3$
β: mean pitch angle at 70% of the blade radius, deg
γ_k: coefficient of the sine series of Γ, m^2/s
Γ: circulation on the blade or the wake, m^2/s
ϑ: angular value associated to ξ, by Eq. 25
μ: norm of the relative velocity on the blade, m/s
ξ: current coordinate along the blade radius, m
ρ: air density, Kg/m^3
τ: thrust coefficient, $\tau = F\pi^2/4\rho\omega^2 r_1^2$
ϕ: functional
χ: power coefficient, $\chi = Q\pi^3/4\rho\omega^2 r_1^5$
ψ: blade azimuth angle
ψ_b: azimuthal periodicity
ψ_s: azimuthal far wake position given by Eq. 3
ω: angular rotational speed, rad/s
Superscripts
$\rightarrow$: denotes vectors of three components
—: denotes vectors of any number of components
Subscripts
i: blade index
n: normal component
j: component index
0: initial value

1 Introduction

The goal of predicting local and overall blade airloads is of crucial importance in developing and improving current propeller blade designs. The capacity of predicting accurately the wake behind rotating blades is also required for the determination of aerodynamic interference effects on the aircraft wing and fuselage (Ardito Marretta, 1994, 1996; Ardito Marretta, Davì, Lombardi, Milazzo, 1997, 1999a, Ardito Marretta, Davì, Lombardi, Milazzo, Carley, 1999b). This is especially true in the case of highly loaded propellers and recently proposed tilt rotors (Ardito Marretta, Davì, Lombardi, Milazzo, 1997). As regards the flowfield generated by isolated propellers and helicopter rotors operating in various flight regimes, analytical models can be classified according to the way in which the vortical structures of the wake and their influence on the blade loading are modeled. In earlier investigations, the geometry of the wake and the vortical structures were prescribed, and the induced velocities needed only to be calculated at the different blade sections. The prescribed geometry is based

[1] Graduate Student, Department of Mechanics and Aeronautics, University of Palermo, Italy
[2] Research Engineer, Department of Mechanics and Aeronautics, University of Palermo, Italy

on empirical modeling laws deduced from such tests as flow visualization, hot-wire and laser velocity measurement techniques (Egolf and Landgrebe, 1983; Elliott, Althoff, Sellers, Nichols, 1987; Favier and Maresca, 1984; Nsi Mba, Meylan, Maresca, Favier, 1984). At low speed, the biggest challenge in predicting the rotor/propeller flowfield is the accurate representation of the vorticity in low-speed forward flight (Berkman, Sankar, Berezin, Torok, 1997). The existing finite difference methodologies for rotor aerodynamics can be divided into two categories, depending on their treatment of wake effects. First generation methods (Caradonna and Tung, 1981; Sankar and Prichard, 1985; Sankar, Wake, Lekoudis, 1986; Agarwal and Desse, 1987; Wake and Sankar, 1989) solved the potential, Euler, or Navier-Stokes equations coupled with an external free or rigid wake model. Second generation Navier-Stokes codes tried to capture the shed vorticity and the tip vortex. This approach needs significant computer resources, even when high order spatial accuracy schemes are used. Although some attempts have been made in the past to reduce computer time through the use of a hybrid (Navier-Stokes/full potential) method (Berezin and Sankar, 1994), in such methods the rotor wake is captured by Eulerian approaches and is not adequately resolved away from the rotor. In order to improve the accuracy of the free vortex-flow prediction, several other investigators have proposed including a free wake that is allowed to assume the geometry corresponding to the bound circulation distribution as determined by the inflow velocities and the blade configuration (planform, airfoil section, twist, tip shape and so on). As a consequence, the solution procedure involves a numerical scheme which includes repeated changes of the wake geometry, until convergence is obtained on bound circulation and performance parameters (Free Wake Analysis) (Summa and Clark, 1979; Caradonna and Tung, 1981; Maresca, Nsi Mba, Favier, 1982; Bliss, Teske, Quackenbush, 1985). Convergence criteria and procedures have been proposed and implemented for experimentally prescribed blade calculations (Maresca, Favier, Nsi Mba, 1986). More recently (Ardito Marretta, 1994, 1996; Ardito Marretta, Davì, Lombardi, Milazzo, 1997, 1999a, Ardito Marretta, Davì, Lombardi, Milazzo, Carley, 1999b, Favier and Maresca, 1984; Favier, Ettaouil, Maresca, 1989; Chiaramonte, Favier, Maresca, Benneceur, 1996), FWA appears to be a very robust and powerful tool to investigate the aerodynamic behaviour and mechanism of rotary wings. At this point, some remarks due to Ribner (Ribner, 1997) are necessary, who provides important guidelines concerning the neglecting of wake roll-up which slightly miscalculates the propeller efficiency. As he elegantly quotes, the underlying scenario goes back to Betz (Betz, 1927), for lightly loaded propellers. Betz showed that this ideal efficiency is associated with an optimum loading that yields a special trailing vortex pattern: one whose induced velocity is such that it behaves like a (multiple) rigid helicoidal sheet or screw surface moving axially backward. Goldstein (Goldstein, 1929) developed the analytical theory and Theodorsen (Theodorsen, 1948) generalized this to apply, allowing for wake contraction, to heavily loaded propellers. He presented rigorous proof that this rigid helicoid wake corresponds to maximum efficiency for his flow model. But the nonrigid behaviour of the wake is a matter that Theodorsen treats rather dismissively, "... the theory [he says] may to some extent be overidealized". The vortex surface is in fact unstable and will therefore not maintain its ideal shape for any lenght of time. When the FWA is employed to model and predict the propeller wake behaviour, good agreement is obtained with experimental data in some flight regimes but large deviation in others, especially for blades with nonlinear twist or sharp evolutive tip shapes. Following references (Maresca, Favier, Nsi Mba, 1986; Johnson, 1986; Landgrebe, 1986), the major discrepancies are due to a still inadequate modeling of the vortex flow generated by a given blade configuration in a given flight regime. The objective of this study is to develop a general multiblade variational scheme, based on a free-wake method, for the prediction of rotor/propeller wake and performance. In this numerical approach, the variational method is applied to solve for the flowfield over a four-bladed propeller in forward flight and at incidence. The variational code presented in this paper is able to successfully resolve three critical aspects of the problem at under consideration: 1) the effects of blade-vortex interactions; 2) the accurate modeling of the initial wake geometry; 3) the evolution and behaviour of the tip vortex size and strength along its path in near wake, which affects the circulation distribution near the blade tip (Chen, Velkoff, Tung, 1987; Favier, Nsi Mba, Barbi, Maresca, 1987). In the present paper, only the forward calculations are considered. The calculations for flight at incidence are currently underway.

2 Mathematical formulation and wake modeling

In this formulation, a free wake model is used to account for wake effects in the regions of flow near to and relatively far from (2 diameters) the propeller. The analytical features of this model not only consider the tip vortex but provide a useful numerical tool to analyze the inboard vortex sheet and the trailed vorticity away from the blade. The method proposed is based on two features which are worth emphasising: 1) the propeller wake need not be prescribed; this allows complete independence from empirical constants; 2) the solution of this aerodynamic problem is reduced to the calculation of a finite number of unknown parameters which are used to minimize a suitable functional. In so doing, full numerical convergence is obtained (divergence may occur in the FWA approach when used in more complex flow configurations). The underlying method goes forward to relevant aspects, a suitable mathematical use of the functional, expressed in terms of the induced velocities, and the procedures to minimize it according to its definite and positive analytical properties. The governing equations of the problem are obtained from a variational principle in which a kinematic functional is employed. A similar approach was in-

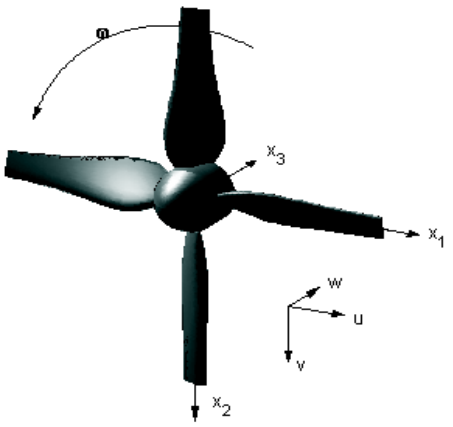

Figure 1 : Propeller fixed coordinate frame ($Ox_1x_2x_3$) and reference system for *u*, *v*, *w*.

troduced by Davì and Milazzo (Davì and Milazzo, 1997) for lateral vibrations of plates in elastodynamics. Their good results have suggested the possible application of the method proposed to the solution of a more complex problem in aerodynamics such as the flowfield of a propeller. Considering a propeller in axial flight, the flow field is steady with respect to a propeller fixed coordinate frame ($Ox_1x_2x_3$) also shown in Fig. 1.

The propeller wake is made up of all the vortex lines starting from points on the blades, for the i-th blade, it is assumed that the vortex sheet parametric equations, in a cylindrical coordinate frame, are expressed as follows:

$$r_i(\psi,\xi,\overline{q}) = \underline{\underline{N}}_{r_i}(\psi,\xi)\cdot\overline{q} + r_{i0}(\psi,\xi) \quad r_0 \le \xi \le r_1 \tag{1}$$

$$z_i(\psi,\xi,\overline{q}) = \underline{\underline{N}}_{z_i}(\psi,\xi)\cdot\overline{q} + z_{i0}(\psi,\xi) \quad 0 \le \psi \le \psi_s \tag{2}$$

where ξ is the current coordinate along the blade radius; the vortex line is identified by its departure point, ξ. The coordinate ψ, the azimuth angle, describes the whole vortex line for given ξ. Following previous works (Ardito Marretta, 1994, 1996; Ardito Marretta, Davì , Lombardi, Milazzo, 1997, 1999a, Ardito Marretta, Davì , Lombardi, Milazzo, Carley, 1999b, Favier and Maresca, 1984; Favier, Ettaouil, Maresca, 1989; Chiaramonte, Favier, Maresca, Benneceur, 1996), the upper limit of ψ is ψ_s, outside this value (far wake) the region of flow becomes unstable because the vortex sheet collapses into a three-dimensional turbulent region. As above mentioned, behind the value of ψ_s the flow became unstable but, anyway, the convection dominance of propeller flow like that of interest here makes this essentially irrelevant. For this reason, here, the influence of the far wake is neglected. According to these authors, ψ_s can be related to the operating parameter j, to the mean pitch angle β (at 70% of blade radius), to the number of blades b, and to the angle between each blade ψ_b, as follows:

$$(\psi_s - \psi_b)/b\psi_b = 0.25\,[8.5 - \beta/10 - j(j+2)] \tag{3}$$

The wake model for propeller flow proposed in this paper is based on a variational principle in which **q** is a vector of unknown parameters. Through the shape matrices, $\mathbf{N}_r$ and $\mathbf{N}_z$, the vector **q** is assumed sufficient to define any sheet geometry; this is more true as the number of components of **q** increases. For **q** equal to zero, one obtains the arbitrary starting shape defined by:

$$r_{0_i}(\psi,\xi) = \xi \quad r_0 \le \xi \le r_1 \tag{4}$$

$$z_{0_i}(\psi,\xi) = \frac{V_\infty}{\omega}\cdot\left[\psi - (i-1)\frac{2\pi}{b}\right] \quad 0 \le \psi \le \psi_s \tag{5}$$

By assuming the blades to be described by a lifting line, through the Biot-Savart law applied to the blade circulation, $\Gamma(\xi)$, and to the trailing wake vortices, the induced velocity at any point **x**, becomes:

$$\vec{V}(\vec{x},\vec{q}) = \frac{1}{4\pi}\sum_{i=1}^{b}\int_{r_0}^{r_1}\Gamma_i\frac{d\vec{y}\wedge(\vec{x}-\vec{y})}{||\vec{x}-\vec{y}||^3} + \frac{1}{4\pi}\sum_{i=1}^{b}\int_{r_0}^{r_1}-\frac{d\Gamma_i}{d\xi}\int_{C_i(\xi,\overline{q})}\frac{d\vec{y}\wedge(\vec{x}-\vec{y})}{||\vec{x}-\vec{y}||^3} \tag{6}$$

where $C_i(\xi,q)$ identifies the generic vortex line. In first approximation the Kutta-Joukowski theorem, at each point on the blade, relates the circulation and the velocity as follows:

$$\Gamma(\xi) = \frac{1}{2}\mu(\xi)\cdot c_l(\xi)\cdot c(\xi) \tag{7}$$

where $\mu(\xi)$ is the local norm of the relative velocity, $c_l(\xi)$ is the local lifting coefficient and $c(\xi)$ the local chord. Eq. 7, through the Eq. 6, becomes an integro-differential equation in $\Gamma(\xi)$, which admits solution for any value of **q**. Among all these possible solutions, only one is "*congruent*" with respect to the impermeable wake condition. According to this condition, the velocity of the fluid,(at the two sides of the wake) with respect to a propeller fixed observer, must be tangent to the wake. If the integral equation in $\Gamma(\xi)$ is obtained, the finite number of components of q does not allow the complete "*congruence*" at all points of the wake (i.e. the analytical structure used cannot rigorously describe all possible wake shapes). Thus, the strategy for obtaining the required "congruence" is to define a generalized condition through the introduction of a functional in such a way that:

$$\phi(\overline{q}) = \int_{r_0}^{r_1}\left(\int_{C_1}(\xi,\overline{q})\,\frac{1}{2}\cdot\left|\left|\vec{V}_n(\vec{x},\overline{q})\right|\right|^2||d\vec{x}||\right)\cdot d\xi \tag{8}$$

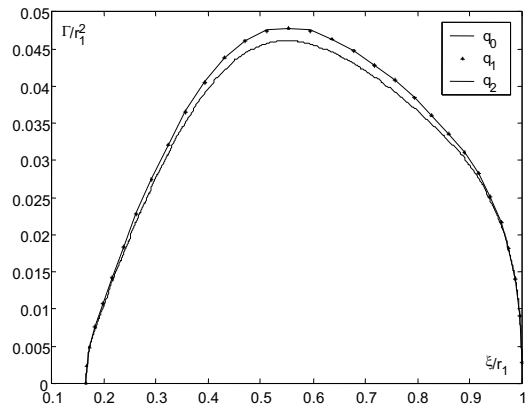

Figure 2 : Circulation distribution along the blade at different values of the iteration steps ($\beta = 27^\circ$ and $j = 0.89$).

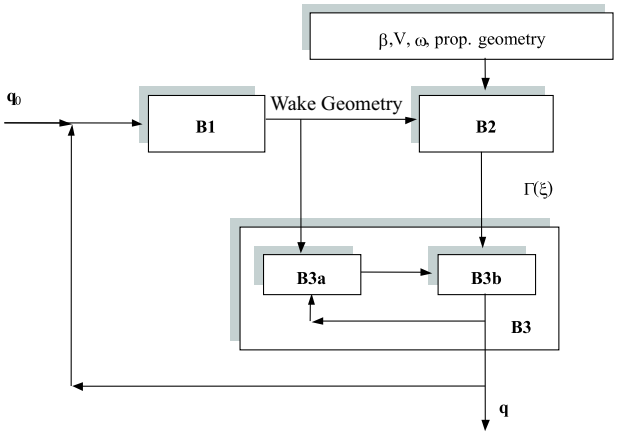

Figure 3 : Block diagram of the recursive computer synthesis for Eq. 12

which depends only from the shape of the wake. In Eq. 8 $\mathbf{V}_n$ can be obtained by observing that the induced velocity at the two sides of the wake, $\mathbf{V}_u$ and $\mathbf{V}_l$ are given by

$$\vec{V}_{u,l} = \vec{V}(\vec{x}, \overline{x}) \pm \frac{\vec{g} \wedge \vec{n}}{2} \tag{9}$$

where the first addend on the right hand is given by Eq. 6 (meaning the principal value of Cauchy) while $\mathbf{g}$ is the local vorticity tangent to the wake. This imply that the normal component of the induced velocity depends only from the term $\mathbf{V}(\mathbf{x}, \mathbf{q})$. Thus called $\mathbf{V}_\tau$ the translation velocity and defining $\mathbf{V}_r$ as:

$$\vec{V}_r = \vec{V}(\vec{x}, \overline{q}) - \vec{V}_\tau \tag{10}$$

one obtains:

$$\vec{V}_n = \vec{V}_r - \vec{V}_r \times \vec{T} \cdot \vec{T} \tag{11}$$

where $\mathbf{T}$ is the versor tangent to the vortex line, $C_1(\xi, \mathbf{q})$; ϕ becomes stationary for the solution, $\mathbf{q}^*$, which satisfies:

$$\frac{\partial \phi(\overline{q}^*)}{\partial q_j} = 0 \quad j \in \{1, 2, \ldots, n_q\} \tag{12}$$

where n_q are the elements of $\mathbf{q}$. Eq. 12 expresses the generalized congruence condition leading to the exact solution obtained when $\phi(\mathbf{q}^*) = 0$.

3 Numerical simulation

The numerical solution of Eq. 12 is strongly simplified by noting that small wake distortions do not produce significant variation in the blade circulation, $\Gamma(\xi)$. Strictly speaking, $\Gamma(\xi)$ depends only weakly on $\mathbf{q}$, as shown in Fig. 2 for different values of $\mathbf{q}$.

Following the block diagram shown in Fig. 3 and starting from the initial value of the functional $\mathbf{q}$, (i.e. $\mathbf{q}_0$ equal to zero), through the $B1$ module, the starting wake geometry is generated. Once the initial propeller wake is modeled, the wake and the operating parameters become the input for the next computational step. At this step, $\mathbf{q}$ is assumed constant and the integral Eq. 7 is then solved with respect to $\Gamma(\xi)$. The function obtained when related to the starting wake geometry, represents the input for the module $B3$, in which the Eq. 12 are processed and solved in terms of $\mathbf{q}$. The sequence of the numerical iterations replace $\mathbf{q}_0$ with $\mathbf{q}$ and enters a recursive computer program. This matches converges when the changes in circulation $\Gamma(\xi)$ become negligible between two iterating steps, i.e. $n-1$ and n.

Continual checking of the functional solution $\mathbf{q}*$ provides good convergence at the first step. In more detail, the wake modeling is based on the analytical expressions for the radial and axial deformations of the propeller wake, Δr and Δz, respectively:

$$\Delta r(\psi, \xi, \overline{q}) = r(\psi, \xi, \overline{q}) - r_0(\psi, \xi) \tag{13}$$

$$\Delta z(\psi, \xi, \overline{q}) = z(\psi, \xi, \overline{q}) - z_0(\psi, \xi) \tag{14}$$

To represent Δr, we assume the following form:

$$\Delta r(\psi, \xi, \overline{q}) = \begin{bmatrix} \psi & \psi^2 & .. & .. & \psi^{nr} \end{bmatrix} \cdot \begin{bmatrix} a_1(\xi) \\ a_2(\xi) \\ .. \\ .. \\ a_{nr}(\xi) \end{bmatrix} \tag{15}$$

where n_r is the degree of the polynomial in ψ and $a_1(\xi)$, $a_2(\xi)$,

$\ldots$, $a_{nr}(\xi)$ are functions given by:

$$a_1(\xi) = \begin{bmatrix} 1 & \xi & .. & .. & \xi^{(m_r-1)} \end{bmatrix} \cdot \begin{bmatrix} p_{l_1} \\ p_{l_2} \\ .. \\ .. \\ p_{l_{m_r}} \end{bmatrix} \tag{16}$$

or, in a more compact form:

$$\underline{\underline{e}}(\xi) = \begin{bmatrix} 1 & \xi & .. & .. & \xi^{(m_r-1)} \end{bmatrix};$$

$$\overline{p}_l = \begin{bmatrix} p_{l_1} \\ p_{l_2} \\ .. \\ .. \\ p_{l_{m_r}} \end{bmatrix} \rightarrow a_l(\xi) = \underline{\underline{e}}(\xi) \cdot \overline{p}_l \tag{17}$$

where m_r is the degree of the polynomial in ξ and p_l is a vector of unknown parameters. Choosing m_r leading filaments, 1, 2, $\ldots$, ξ_{m_r} and writing the following:

$$\overline{q}_l = \begin{bmatrix} a_1(\xi_1) \\ a_2(\xi_2) \\ .. \\ .. \\ a_1(\xi_{m_r}) \end{bmatrix} \in M_{m_r \times l}; \quad \underline{\underline{E}} = \begin{bmatrix} \underline{\underline{e}}(\xi_1) \\ \underline{\underline{e}}(\xi_2) \\ .. \\ .. \\ \underline{\underline{e}}(\xi_{m_r}) \end{bmatrix} \in M_{m_r \times m_r} \tag{18}$$

Eq. 17 and Eq. 18 lead to:

$$\overline{q}_l = \underline{\underline{E}} \cdot \overline{p}_l \rightarrow a_l(\xi) = \underline{\underline{e}}(\xi) \cdot \underline{\underline{E}}^{-1} \cdot \overline{q}_l \tag{19}$$

by writing again:

$$\underline{\underline{\Lambda}}(\xi) = \begin{bmatrix} \underline{\underline{e}}(\xi) \cdot \underline{\underline{E}}^{-1} & \underline{\underline{0}} & .. & .. & \underline{\underline{0}} \\ \underline{\underline{0}} & \underline{\underline{e}}(\xi) \cdot \underline{\underline{E}}^{-1} & .. & .. & \underline{\underline{0}} \\ .. & .. & .. & .. & .. \\ .. & .. & .. & .. & .. \\ \underline{\underline{0}} & \underline{\underline{0}} & .. & .. & \underline{\underline{e}}(\xi) \cdot \underline{\underline{E}}^{-1} \end{bmatrix} \in M_{n_r \times (n_r \cdot m_r)} \tag{20}$$

$$\overline{q} = \begin{bmatrix} \overline{q}_1 \\ \overline{q}_2 \\ .. \\ .. \\ \overline{q}_{n_r} \end{bmatrix} \in M_{(m_r \cdot n_r) \times l} \tag{21}$$

the Eq. 15 becomes:

$$\Delta r(\psi, \xi, \overline{q}) = \begin{bmatrix} \psi & \psi^2 & .. & .. \psi^{n_r} \end{bmatrix} \cdot \underline{\underline{\Lambda}}(\xi) \cdot \overline{q} \tag{22}$$

and from Eq. 22, by definition:

$$\underline{\underline{N}}_r(\psi, \xi) = \begin{bmatrix} \psi & \psi^2 & .. & .. & \psi^{n_r} \end{bmatrix} \cdot \underline{\underline{\Lambda}}(\xi) \tag{23}$$

A similar technique is used for Δz.

The integral equation Eq. 7 is replaced by a system of n algebraic equations in n unknown parameters Γ_k, which represent the coefficients of the blade circulation expressed by a sine series, i.e.:

$$\Gamma(\vartheta_\xi) = \sum_{k=1}^{n} \gamma_k \sin(k\vartheta_\xi) \tag{24}$$

where ϑ_ξ is related to ξ by the (well-known) relation:

$$\xi = \frac{r_1 + r_0}{2} + \frac{r_1 - r_0}{2} \cos(\vartheta_\xi) \tag{25}$$

The set of n equations is based on writing the equation Eq. 7 in n points of the blade, which were previously fixed through the Multhopp formula. This method does not need to neglecting the contribution of the blade tip and the propeller hub region. For the s-th point one obtains:

$$\vartheta = \frac{s\pi}{n+1} \tag{26}$$

At any point, now fixed by ϑ_x, the *j-th* component of the induced velocity may be written as:

$$V_j = \frac{1}{4\pi} \int_0^\pi \frac{d\Gamma}{d\vartheta_\xi} \cdot \frac{G_j(\vartheta_x, \vartheta_\xi)}{\cos(\vartheta_\xi) - \cos(\vartheta_x)} d\vartheta_\xi \tag{27}$$

where $G_j(\vartheta_x, \vartheta_\xi)$ is the influence function defined as follows:

$$G_j(\vartheta_x, \vartheta_\xi) = (\cos(\vartheta_\xi) - \cos(\vartheta_x)) \cdot \sum_{i=1}^{b} \int_{C_i(\vartheta_\xi, \overline{q})} \left(\frac{d\vec{y} \wedge (\vec{x} - \vec{y})}{||\vec{x} - \vec{y}||^3} \right)_j \tag{28}$$

where **x** is the vector associated with ϑ_x, and the difference term $\cos(\vartheta_\xi) - \cos(\vartheta_x)$ removes the singularity which occurs when ϑ_ξ tends toward ϑ_x. Thus, $G_j(\vartheta_x, \vartheta_\xi)$ may be expressed by the cosine series written below:

$$G_j(\vartheta_x, \vartheta_\xi) = \sum_{h=1}^{m} g_{j,h}(\vartheta_x) \cos((h-1)\vartheta_\xi) \tag{29}$$

The coefficients $g_{j,h}(\vartheta_x)$, for given ϑ_x, are obtained evaluating the relation Eq. 28 at m points ϑ_ξ, chosen via the expression Eq. 26 and solving the system obtained by the equation Eq. 29 written with respect to $g_{j,h}$. Fig. 4 shows the function $G_j(\vartheta_x, \vartheta_\xi)$ for a single blade and a given operating condition; from the reported results it is easy to deduce that the singularities have been removed and replaced by discontinuities of the first kind which are quite well approximated by the cosine series.

Eq. 27, through the relations Eq. 24 and Eq. 29, can be rewritten as:

$$V_j(\vartheta_x) = \sum_{k=1}^{n} \sum_{h=1}^{m} \frac{\gamma_k k g_{j,h}(\vartheta_x)}{4\pi} \int_0^\pi \frac{\cos(k\vartheta_x)\cos((h-1)\vartheta_\xi)}{\cos(\vartheta_\xi) - \cos(\vartheta_x)} d\vartheta_\xi \tag{30}$$

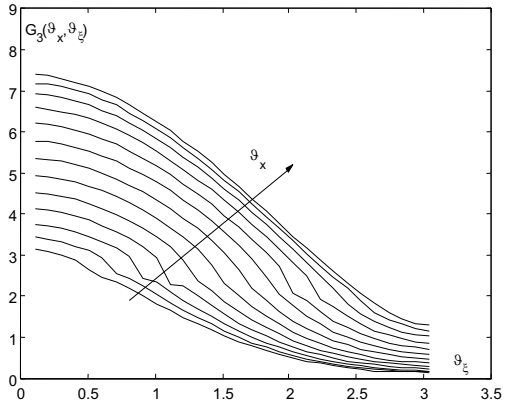

Figure 4 : Influence function related to one blade.

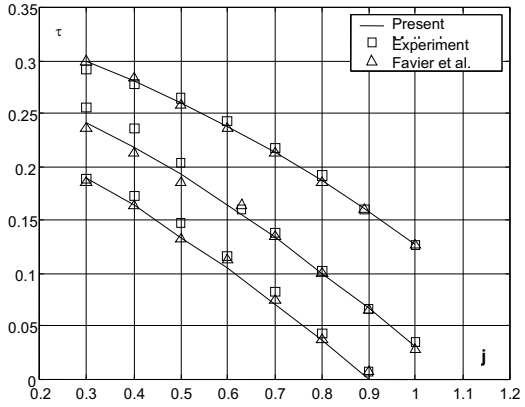

Figure 5 : Propeller thrust coefficient

moreover, the integral in the right hand term can be solved by Glauert's formula

$$V_j(\vartheta_x) = \sum_{k=1}^{n}\sum_{h=1}^{m} \frac{\gamma_k k g_{j,h}(\vartheta_x)}{8\sin(\vartheta_x)} \times \left[\sin(|k+h-1|\vartheta_x) + \sin(|k-h+1|\vartheta_x)\right] \tag{31}$$

by writing:

$$f_{jk} = \sum_{h=1}^{m} \frac{k g_{j,h}(\vartheta_x)}{8\sin(\vartheta_x)} \left[\sin(|k+h-1|\vartheta_x) + \sin(|k-h+1|\vartheta_x)\right] \tag{32}$$

associated with the following matrix notation:

$$\underline{\underline{f}}_j = \begin{bmatrix} f_{j,1} & f_{j,2} & .. & .. & f_{j,n} \end{bmatrix}, \quad \overline{\gamma} = \begin{bmatrix} \gamma_1 \\ \gamma_2 \\ .. \\ .. \\ \gamma_n \end{bmatrix} \tag{33}$$

the previous equation Eq. 31 leads to:

$$V_j(\vartheta_x) = \underline{\underline{f}}_j(\vartheta_x) \cdot \overline{\gamma} \tag{34}$$

Eq. 34 allows to calculate in each points ϑ_x the local blade lift coefficient $c_l(\xi)$, and the local relative velocity, and then the right hand term of the equation Eq. 7. The system so obtained is solved through the Newton-Raphson method. The described procedure is applied to find the solution of the system of equations Eq. 12 which becomes an algebraic set of equations, via the hypothesis of no-correlation between $\Gamma(\xi)$ and $\mathbf{q}$.

The iteration is executed by the sub-modules *B*3*a* and *B*3*b* so that, at the step *s*, sub-module *B*3*a* generates the wake geometry associated with the value of $\mathbf{q}$ related to that calculation step, i.e. $\mathbf{q}^s$. Note that the model used is the same as employed in *B*1.

Inside the module *B*3 the partial derivatives of $\mathbf{q}$, for $\mathbf{q} = \mathbf{q}^s$, are calculated by writing:

$$\underline{\underline{H}} = \begin{bmatrix} \frac{\partial^2\phi}{\partial q_1^2} & \frac{\partial^2\phi}{\partial q_1 \partial q_2} & .. & .. & \frac{\partial^2\phi}{\partial q_1 \partial q_{n_q}} \\ \frac{\partial^2\phi}{\partial q_1 \partial q_2} & \frac{\partial^2\phi}{\partial q_2^2} & .. & .. & \frac{\partial^2\phi}{\partial q_2 \partial q_{n_q}} \\ .. & .. & .. & .. & .. \\ \frac{\partial^2\phi}{\partial q_{n_q} \partial q_2} & \frac{\partial^2\phi}{\partial q_{n_q} \partial q_2} & .. & .. & \frac{\partial^2\phi}{\partial q_{n_q}^2} \end{bmatrix} \quad \overline{d} = \begin{bmatrix} \frac{\partial\phi}{\partial q_1} \\ \frac{\partial\phi}{\partial q_2} \\ .. \\ .. \\ \frac{\partial\phi}{\partial q_{n_q}} \end{bmatrix} \tag{35}$$

$\mathbf{q}$ at the next step $s+1$, is given by:

$$\overline{q}^{s+1} = \overline{q}^s - \underline{\underline{H}}^{-1}\overline{d} \tag{36}$$

the iteration process stops when the error function defined as:

$$error = \max\left\{ \left|q_1^{s+1} - q_1^s\right|, \left|q_2^{s+1} - q_2^s\right|, .., .., \left|q_{n_q}^{s+1} - q_{n_q}^s\right| \right\} \tag{37}$$

becomes relatively small or negligible.

The sequence of the numerical approach starts to calculate the derivatives of $r(\psi, \xi, q)$ and $z(\psi, \xi, q)$ as their analytical expressions are known. The induced velocity derivatives are given by Eq. 28 and Eq. 31, where now $\mathbf{x}$ is the local point at which the velocity is calculated, $\mathbf{x}$ belonging to the vortical filament trailing from the point of the blade ϑ_x, while ϑ_y identifies the shedding point of the filament which inducing a velocity at $\mathbf{x}$.

4 Results and discussions

The numerical method has been tested on the propeller shown in Fig. 1, for which Favier has made detailed measurements.

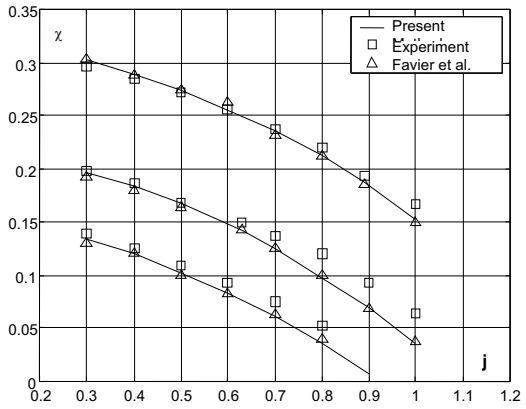

Figure 6 : Propeller torque coefficient

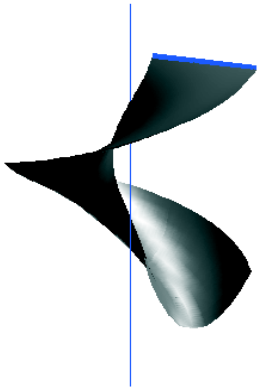

Figure 7 : Blade vortex related to q_2 ($\beta = 23°$, $j = 0.70$).

The model tested consists of a four-bladed propeller having diameter $D = 0.85\,m$ (hub diameter, $D_0 = 0.14\,m$). The blades are constituted by the NACA 64A408 airfoil series with a non linear twist law (Ardito Marretta, Davì, Lombardi, Milazzo, 1997). Further details will be found on Ref. (Favier, Ettaouil, Maresca, 1989).

The three-dimensional numerical simulation code of a propeller in axial flight was validated by comparing the present computations with results in literature. In Fig. 5 and 6 are shown measured and calculated performance characteristics, obtained for the propeller operating parameter variable within the range $0.3 \leq j \leq 1.0$ and for three different values of the mean pitch angle, β.

The same figures display the numerical results of Favier, Ettaouil, Maresca, (1989) obtained by the FWA approach which made use of some empirical constants to adequately model the

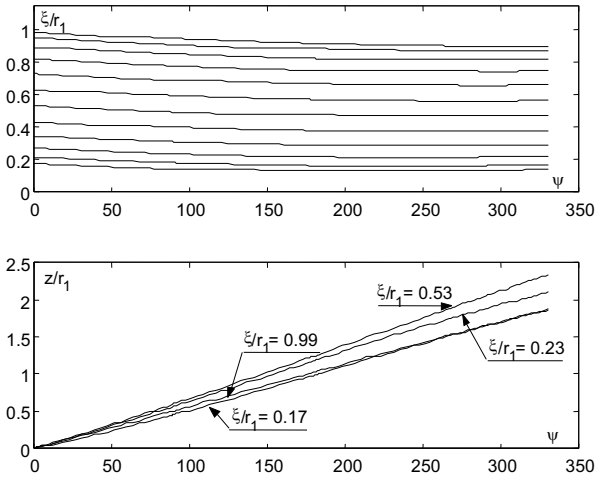

Figure 8 : (i) wake vortex filaments radius evolution against azimuth (*deg*); (ii) Four wake filaments in axial evolution against azimuth (*deg*). (Only 4 filaments are displayed for clearness)

propeller wake. Overall good agreement of both the two series of calculation validates our modeling approach in the simulation of the tractor propeller flow.

The conditions examined in the procedure validation included the same airfoil aerodynamic characteristics (c_d, c_l) of the previously quoted reference for a fixed Reynolds number (about 10^6). The slight theoretical underestimation of the power coefficient, which occurs for $j \leq 0.6$, is due to the increased drag coefficient at increased Reynolds-number. For these values of j, the Reynolds-number becomes about five times greater than the chosen value, causing a significant variation in c_d, which underestimated results compared to those with $R_e = 10^6$.

Due to the nature of the defined functional, which can be thought of as a mean square error, via the minimization of $\phi(x)$, the formulation yields overall accurate predictions. As a consequence, the numerical results for the overall parameters of the propeller, such as torque and thrust, flowing therefrom became appropriate values leading to the conclusion that the variational approach presented here substantially may not be over-or underpredicting substantially.

Fig. 7 displays the shape of a single vortex sheet shedding from the trailing edge of the blade when modeled by the vector **q** from calculations with $\beta = 23°$ and $j = 0.70$. In Fig. 8(i,ii) are represented the wake filaments evolution along the radial and axial directions, respectively. Fig. 9 shows the matching of the convergence through the initial wake shape untill the final geometrical step is reached.

Finally, in Fig. 10 and 11 are presented the maps of the velocity

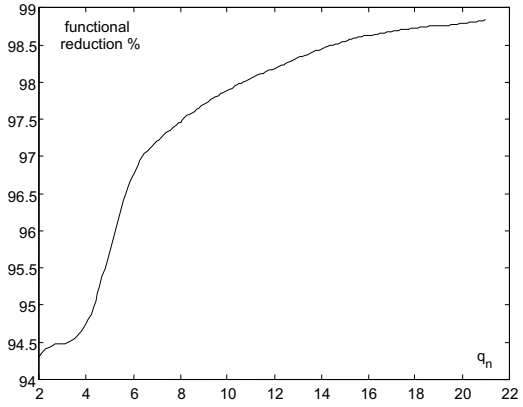

Figure 9 : Functional reduction against component n_q of **q** (the reduction is compared to the corresponding **q** value of the wake initial shape).

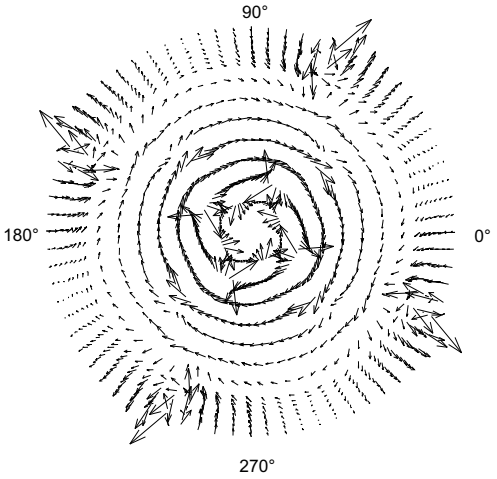

Figure 11 : Map a of the velocity components lying on a disc positioned at $1.181r_1$ behind the propeller ($\beta = 27^\circ$ and $j = 0.63$).

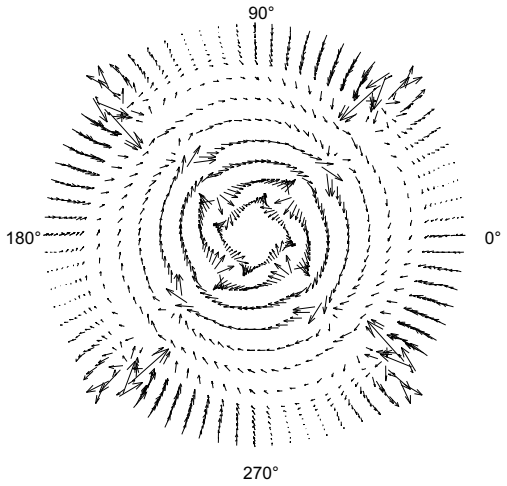

Figure 10 : Map a of the velocity components lying on a disc positioned at $0.231r_1$ behind the propeller ($\beta = 27^\circ$ and $j = 0.63$).

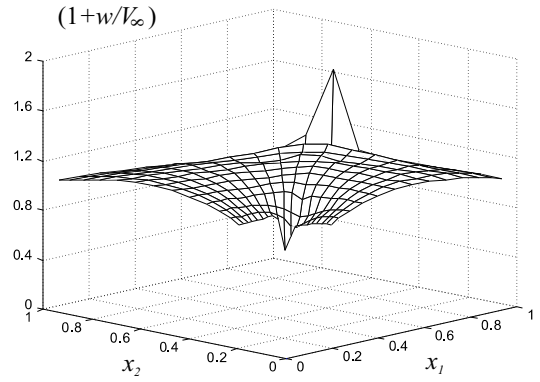

Figure 12 : Map a of the relative velocity (axially directed) on a quarter of a disc positioned at $0.231r_1$ behind the propeller ($\beta = 32.5^\circ$ and $j = 0.89$).

component lying on two discs downstream the propeller, at $0.23r_1$ and $1.181r_1$, respectively. They are in good agreement with those of Favier and co-authors.

Meanwhile, Fig. 12 shows the velocity component parallel to the propeller axis.

5 Conclusions

A numerical investigation using a variational approach of the complex aerodynamic problem of the flowfield of a four-bladed propeller has been performed in an attempt to enhance the currently available methods. This variational procedure is conducted without the constraint of maintaining a prescribed propeller wake geometry. Code correlation with experimental-tests data for the current system, for the same operating conditions, is satisfectory. Even though the propeller is considered in forward flight, the variational formulation discussed here could be adapted to the more complex problem involving non-periodic variables including nonlinear vibrations and noise transmission.

Acknowledgement: The authors would like to acknowledge the contribution of Giuseppe Davì and Alberto Milazzo of the Department of Mechanics and Aeronautics of Palermo (Italy) for many helpful discussions. We are also grateful and indebted to Michael Carley of Trinity College, Dublin (Ire-

land) for his superb, practical help in the preparation of this paper.

References

Agarwal, R. K.; Desse, J. E. (1987): Euler calculations for flowfield of a helicopter rotor in hover. *AIAA Journal of Aircraft*, vol. 24, pp. 231–238.

Ardito Marretta, R. M. (1996): Performance of a propeller embedded in the flowfield of a wing. *AIAA Journal of Aircraft*, vol. 5, pp. 919–923.

Ardito Marretta, R. M.; Davi', G.; Lombardi, G.; Milazzo, A. (1997): Wing-propeller coupling simulation from tractor up to hover flight conditions. *Computer Modeling and Simulation in Engineering*, vol. 2, pp. 304–321.

Ardito Marretta, R. M.; Davi, G.; Lombardi, G.; Milazzo, A. (1999): Hybrid numerical technique for evaluating wing aerodynamic loading with propeller interference. *Computers & Fluids*, vol. 8, pp. 923–950.

Ardito Marretta, R. M.; Davi, G.; Lombardi, G.; Milazzo, A.; Carley, M. (1999): Simulation model and computation of noise emission of an installed propeller. *Computer Modeling and Simulation in Engineering*, vol. 4, pp. 104–116.

Ardito Marretta, R. M.; Lombardo, G. (1994): Coefficienti di trazione, di coppia e rendimento dell'elica in presenza del campo aerodinamico di un'ala finita. *Aerotecnica - Missili e Spazio*, vol. 1-2, pp. 31–41.

Berezin, C. R.; Sankar, L. N. (1994): An improved Navier-Stokes full potential coupled analysis for rotors. *Mathematical Computational Modeling*, vol. 19, pp. 125–133.

Berkman, M. E.; Sankar, L. N.; Berezin, C. R.; Torok, M. S. (1997): Navier-Stokes/full potential/free-wake method for rotor flows. *AIAA Journal of Aircraft*, vol. 5, pp. 635–640.

Betz, A. (1927): Screwpropeller with least energy loss. *Göttinger Nachrichten*, vol. 1919, pp. 193–213 (in German), also reprinted in Vier Abhandlungen zur hydrodynamik und aerodynamik, Göttingen, Germany, 1927, pp. 68–92.

Bliss, D. B.; Teske, M. E.; Quackenbush, T. R. (1985): Free-wake calculations using curved vortex elements. In *Proceedings of the 1th International Conference on rotor basic research*, pp. 1–22. Research Triangle Park (USA).

Caradonna, F. X.; Tung, C. (1981): Experimental analytical studies of a model helicopter rotor in hover. *Vertica*, vol. 5, pp. 149–161.

Chen, C. S.; Velkoff, H. R.; Tung, C. (1987): Free-wake analysis of a rotor in hover. *AIAA paper*, pp. 87–1245.

Chiaramonte, J. Y.; Favier, D.; Maresca, C.; Benneceur, S. (1996): Aerodynamic interaction study of the propeller/wing different configurations. *AIAA Journal of Aircraft*, vol. 1, pp. 46–53.

Davi', G.; Milazzo, A. (1997): A new symmetric and positive definite boundary element formulation for lateral vibrations of plates. *Journal of Sound and Vibration*, vol. 206, pp. 507–521.

Egolf, T. A.; Landgrebe, A. J. (1983): Helicopter rotor wake geometry and its influence in forward flight. *Nasa CR*, vol. 1-2, pp. 3726–3727.

Elliott, J. W.; Althoff, S. L.; Sellers, W. L.; Nichols, C. E. (1987): Inflow velocity measurements made on an helicopter rotor using a two-component laser velocimeter. *AIAA Paper*, pp. 87–1321.

Favier, D.; Ettaouil, A.; Maresca, C. (1989): Numerical and experimental investigation of isolated propeller wakes in axial flight. *AIAA Journal of Aircraft*, vol. 9, pp. 837–846.

Favier, D.; Maresca, C. (1984): Etude du sillage 3d d'une hélice aérienne quadripale. *AGARD FDP on Aerodynamics and Acoustics of Propellers*, vol. 15, pp. CP–366.

Favier, D.; Nsi Mba, M.; Barbi, C.; Maresca, C. (1985): A free-wake analysis for hovering rotors and advancing propellers. In *Proceedings of the 11th European Rotorcraft Forum*. London, Paper 21. See also (1987): Vertica, vol. 11, pp. 493-511.

Goldstein, S. (1929): On the vortex theory of screw propellers. In *Proceedings of the Royal Society*, volume 123, pp. 440–465.

Johnson, W. (1986): Recent developments in rotary wing aerodynamic theory. *AIAA Journal*, vol. 24, pp. 1219–1244.

Landgrebe, A. J. (1986): Overview of helicopter wake and airloads technology. In *Proceedings of the 12th European rotorcraft forum*, pp. 18.1–18.21. Garmisch-Partenkirchen.

Maresca, C.; Favier, D.; Nsi Mba, M. (1986): A prescribed radial circulation distribution of a hovering rotor blade. In *Proceedings of the 12th European rotorcraft forum*, pp. 23.1–23.25. Garmisch-Partenkirchen.

Maresca, C.; Nsi Mba, M.; Favier, D. (1982): Prediction et vérification du champ des vitesses d'un rotor en vol stationnaire. *AGARD FDP on Aerodynamic Loads on rotorcarft*, vol. 7, pp. CP–334.

Nsi Mba, M.; Meylan, C.; Maresca, C.; Favier, D. (1984): Radial distribution circulation of a rotor in hover measured by laser velocimeter. *Proceedings of the 35th Annual American Helicopter Society Forum*.

Ribner, H. (1997): Neglect of wake roll-up in Theodorsen's theory of propellers. *AIAA Journal of Aircraft*, vol. 34, pp. 814–816.

Sankar, L. N.; Prichard, D. (1985): Solution of transonic flow past rotor blades using the conservative full potential equation. *AIAA Paper*, pp. 85–5012.

Sankar, L. N.; Wake, B. E.; Lekoudis, S. G. (1986): Solution of the unsteady Euler equations for fixed and rotor wing configurations. *AIAA Journal of Aircraft*, vol. 23, pp. 283–289.

Summa, J. M.; Clark, D. R. (1979): A lifting surface method for hover/climb airloads. In *Proceedings of the 35th Annual American Helicopter Society Forum*. Washington D.C. (USA).

Theodorsen, T. (1948): *Theory of Propellers*. Mc Graw-Hill, New York.

Wake, B. E.; Sankar, L. N. (1989): Solution of Navier-Stokes calculations of hovering rotor flowfileds. *Journal of the American Helicopter Society*, vol. 34, pp. 13–22.